

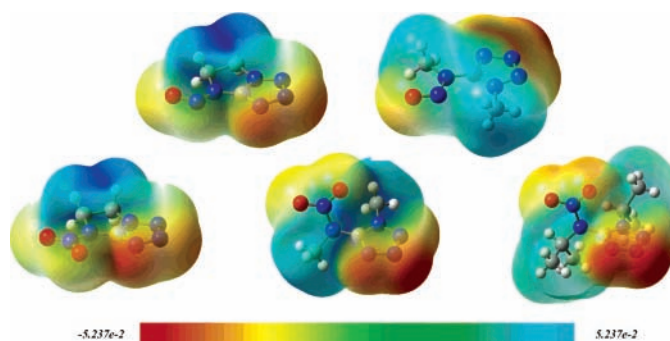
***N*-Nitroso- and *N*-Nitraminotetrazoles**

Konstantin Karaghiosoff, Thomas M. Klapötke,* Peter Mayer,† Holger Piotrowski,†
Kurt Polborn,† Rodney L. Willer, and Jan J. Weigand‡

Department of Chemistry and Biochemistry, Ludwig-Maximilian University Munich, Butenandtstrasse 5-13
(Haus D), 81377 Munich, Germany

tmk@cup.uni-muenchen.de

Received July 4, 2005



N-Nitroso- (**5a,c**) and *N*-nitraminotetrazoles (**6a–c**) were synthesized from the corresponding aminotetrazoles (**3a–c**) either by the direct nitration with acetic anhydride/HNO₃ or by dehydration of the corresponding nitrates (**4a–c**) with concentrated sulfuric acid. The conversion of the *N*-nitrosoaminotetrazoles (**5a,c**) with peroxytrifluoroacetic acid (CF₃CO₃H) yielded the corresponding nitramines in high yield (**6a** (82%), **6c** (80%)). The *N*-nitroso- (**5a,c**) and *N*-nitraminotetrazoles (**6a–c**) have been fully characterized by vibrational (IR, Raman) and multinuclear NMR spectroscopy (¹⁴N/¹⁵N, ¹H, ¹³C), mass spectrometry, and elemental analysis. A detailed discussion of the ¹⁵N chemical shifts and ¹H–¹⁵N coupling constants is given. The molecular structures in the solid state were determined by single-crystal X-ray diffraction (**3a,c**; **5a,c**; **6a–c**) and a detailed discussion of the molecular structures will be presented. Furthermore, the structure and bonding as well as N,N rotational barriers are discussed on the basis of theoretically obtained data (B3LYP/6-31G(d,p), NBO analysis). In the case of two *N*-nitraminotetrazoles (**6a,c**) the physicochemical properties (e.g., *D*, *P*, Δ_fH°) were evaluated. The heat of formation was calculated to be positive for **6a** and **6c** (+2.8 and +85.2 kcal mol⁻¹, respectively) and the calculated detonation velocity with 5988 (**6a**) and 7181 (**6c**) m s⁻¹ reaches values of TNT and nitroglycerin.

Introduction

An ideal explosive is powerful, safe, and easy to handle; can be stockpiled for long periods in any climate; and is hard to detonate except under precisely specified conditions. The history of high explosives goes back to 1885, when the first high explosive, 2,4,6-trinitrophenol (picric acid),¹ was put into service in France. As the result of some disadvantages of this compound, i.e., high melting point, reaction with metals, and high sensitivity, it was replaced by another less sensitive high explosive,

2,4,6-trinitroloouene (TNT);² this compound is still used today in explosive mixtures. The next generation of higher performance explosives are the nitramine compounds hexahydro-1,3,5-trinitro-*S*-triazine (RDX)³ and octahydro-1,3,5,7-tetranitro-1,3,5,7-tetrazine (HMX)⁴ (Figure 1). In the pure state these compounds are too sensitive and can only be used with insensitive additives or in mixtures.

† X-ray structure analysis.

‡ Dalhousie University, B3H 4J3 Halifax, NS Canada.

(1) Köhler, J.; Meyer, R. *Explosivstoffe*, 9. Aufl.; Wiley-VCH: Weinheim, Auflage, 1998.

(2) Engineering Design Hand Book: *Properties of Explosives of Military Interest*, Army Material Command, AMC Pamphlet AMCP 706-117; January 1971.

(3) Deal, W. E. *J. Chem. Phys.* **1957**, 27(1), 796.

(4) Mader, C. L. Report LA-2900, Los Alamos Scientific Laboratory; Fortran BKW Code for Computing the Detonation Properties of Explosives; Los Alamos, NM, July 1963.

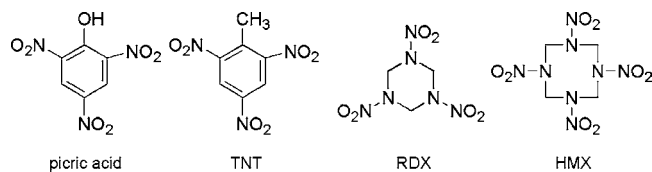


FIGURE 1. Structures of commonly used explosives.

The search for new energetic compounds with increased performance is progressing relatively slowly. The development trends of “New Products” is focused on the manufacturing of blended and polymer-bounded explosives that meets the desired demands of easy processing and handling, while keeping a high security level. Currently much effort is made in order to increase the safety of the explosive products on handling, in case of fire or under other unwanted external influences such as impact, falling, and being fired upon.

In continuation of our studies on compounds with a high nitrogen content, we are currently investigating the chemistry of aminotetrazole derivatives with respect to their use as components in propellants and explosives.^{5,6} Our interests are focused on solid crystalline high energetic materials, made up either of a salt or of neutral molecules. Aminotetrazole derivatives, an increasingly popular functionality with wide-ranging applications,⁷ can be readily converted to the corresponding *N*-nitroso- and *N*-nitraminotetrazoles. They are of interest since they have two energetic sites: the nitroso/nitramino and the tetrazole moieties. Particularly *N*-nitraminotetrazoles are of interest, as they may be used as modifiers for the combustion rates of rocket propellants, as cool gas generators, or as other special explosives such as these investigated by Willer et al.⁸

In comparison to the ionic nitraminotetrazole salts^{9a,b} not much attention has been given to energetic materials based on neutral nitraminotetrazoles, and important data, such as NMR data and crystal structure analysis, are missing for previously published compounds.^{8,9c} Therefore the investigation of the chemistry of simple alkyl-substituted nitraminotetrazoles, especially with respect to NMR data (¹⁵N), crystal structures, N,N rotational barriers around the N–N bond, and different synthetic routes, is the purpose of our contribution. The synthesis in all

cases is based on the conversion of the easily accessible *N*-aminotetrazoles,¹⁰ either by the direct nitration with nitrating agents (e.g., acetic anhydride/HNO₃) or by dehydration of the corresponding nitrates with concentrated sulfuric acid.¹¹ The direct conversion of easily accessible *N*-nitrosaminotetrazoles to the corresponding nitramines by the action of peroxytrifluoroacetic acid, yielding the corresponding pure secondary nitramines, was also investigated. *N*-Nitrosamines exhibit strong carcinogenic and mutagenic properties and are potential NO[•]/NO⁺ donors¹² through homolytic and heterolytic cleavage of the N–NO bond, respectively. For *N*-nitrosaminotetrazoles similar properties should be expected. This class of compounds is only little investigated, however.^{13,14} Here we report the synthesis, multinuclear NMR data, and the molecular structures in the crystal of *N*-nitrosaminotetrazoles (**5a,c**) also. The NMR data and molecular structures of the new nitroso compounds are compared to those of the corresponding *N*-nitraminotetrazoles (**6a–c**).

Results and Discussion

The nitroso- (**5a,c**) and nitraminotetrazoles (**6a–c**) were prepared starting from the corresponding substituted 5-aminotetrazoles. The syntheses of the 5-aminotetrazoles belong to one of the following four main reaction types: (1) amino group or ring functionalization of 5-aminotetrazoles,^{15,16} which often results in mixtures of isomers;^{17,18} (2) substitution of a leaving group in the tetrazole 5-position with amines;¹⁹ (3) various azide-mediated tetrazole ring formation reactions (e.g., from cabodimides,²⁰ cyanamides,²¹ or α -chloroformamidines²²); and (4) reaction of aminoguanidine derivatives with sodium nitrite under acidic conditions.^{23,22a} The latter reaction is the most convenient for the synthesis of the corresponding symmetric substituted 1-methyl-5-(methylamino)-1*H*-tetrazole (**3a**), 1-isopropyl-5-(isopropylamino)-1*H*-tetrazole (**3b**), and 5,6-dihydro-7*H*-imidazolo[1,2-*d*]tetrazole (**3c**). Compounds **3a–c** were obtained according

(5) (a) Hammerl, A.; Holl, G.; Kaiser, M.; Klapötke, T. M.; Mayer, P.; Nöth, H.; Piotrowski, H.; Suter, M. *Z. Naturforsch.* **2001**, *56b*, 857. (b) Hammerl, A.; Holl, G.; Klapötke, T. M.; Mayer, P.; Nöth, H.; Piotrowski, H.; Warchhold, M. *Eur. J. Inorg. Chem.* **2002**, *4*, 834. (c) Geith, J.; Klapötke, T. M.; Weigand, J.; Holl, G. *Propellants, Explos., Pyrotech.* **2004**, *29* (1), 3. Klapötke, T. M.; Mayer, P.; Schulz, A.; Weigand, J. *J. Propellants, Explos., Pyrotech.* **2004**, *29*(5), 325.

(6) (a) Klapötke, T. M.; Mayer, P.; Schulz, A.; Weigand, J. *J. Am. Chem. Soc.* **2005**, *127*, 2032. (b) Gálvez-Ruiz, J. C.; Holl, G.; Karaghiosoff, K.; Klapötke, T. M.; Löhnhwiz, K.; Mayer, P.; Nöth, H.; Polborn, K.; Rohbogner, C. J.; Suter, M.; Weigand, J. *J. Inorg. Chem.* **2005**, *44* (12), 4237. (c) Fischer, G.; Holl, G.; K.; Klapötke, Weigand, J. *J. Thermochim. Acta* **2005**, *437*, 168.

(7) Butler, R. N. In *Comprehensive Heterocyclic Chemistry*; Katritzky, A. R., Rees, C. W., Scriven, E. F. V., Eds.; Pergamon: Oxford, U.K., 1996; Vol. 4.

(8) (a) Willer, R. L. *Synthesis of High-Nitrogen Content Heterocyclic Nitramines and Energetic Internal Plasticizers, Technical Report*, ADA182898, Morton Thiokol, Elkton, **1987**. (b) Brill, T. B. *Proceedings of NATO-ASI on Chemistry and Physics of the Molecular Processes in Energetic Materials*; Bulusu, S. N., Eds.; Kluwer Academic Publisher: Dordrecht, Netherlands, 1989; p 277.

(9) (a) Poole, D. R.; Kwong, P. C. U.S. Patent 5,386,775, 1995. (b) Mayants, A. G.; Klimenko, V. S.; Erina, V. V.; Pyreseva, K. G.; Gordeichuk, S. S.; Leibzon, V. N.; Kuz'min, V. S.; Burtsev, Yu. N. *Khim. Geterot. Soed.* **1991**, *8*, 1067. (c) Gao, A.; Rheingold, A. L.; Brill, T. B. *Propellants, Explos., Pyrotech.* **1991**, *16* (3), 97.

(10) Katritzky, A. R.; Rogovoy, B. V.; Kovalenko, K. V. *J. Org. Chem.* **2003**, *68*, 4941 and references therein.

(11) (a) Willer, R. L.; Henry, R. A. *J. Org. Chem.* **1988**, *53*, 5371. (b) Butler, R. N.; Scott, F. L. *J. Org. Chem.* **1966**, *31*, 3182.

(12) (a) Loeppky, R. N.; Outram, J. R. *N-Nitroso Compounds: Occurrence and Biological Effects*; IARC Scientific Publisher: Lyon, 1982. (b) Wang, P. G.; Xian, M.; Tang, X.; Wu, X.; Wen, Z.; Cai, T.; Janczuk, J. *Chem. Rev.* **2002**, *102*, 1091.

(13) (a) Butler, R. N.; Lambe, T. L.; Tobin, J. C.; Scott, F. L. *J. Chem. Soc., Perkin Trans. 1* **1973**, 1357. Catton, R.; Butler, R. N. *Can. J. Chem.* **1974**, *52*, 1248.

(14) Garrison, J. A.; Herbst, R. M. *J. Org. Chem.* **1956**, *21*, 988.

(15) Ford, R. E.; Knowles, P.; Lunt, E.; Marshall, S. M.; Penrose, A. J.; Ramsden, C. A.; Summers, A. J. H.; Walker, J. L.; Wright, D. E. *J. Med. Chem.* **1986**, *29*, 538.

(16) (a) Peet, N. P. *J. Heterocycl. Chem.* **1987**, *24*, 223. (b) Kato, T.; Chiba, T.; Daneshtalab, M. *Chem. Pharm. Bull.* **1976**, *24*, 2549.

(17) Andrus, A.; Partridge, B.; Heck, J. V.; Christensen, B. G. *Tetrahedron Lett.* **1984**, *25*, 911.

(18) Butler, R. N.; Scott, F. L. *J. Org. Chem.* **1966**, *31*, 3182.

(19) (a) Klich, M.; Teutsch, G. *Tetrahedron* **1986**, *42*, 2677. (b) Barlin, G. B. *J. Chem. Soc. B* **1967**, 641.

(20) (a) Percival, D. F.; Herbst, R. M. *J. Org. Chem.* **1957**, *22*, 925. (b) Ding, Y.-X.; Weber, W. P. *Synthesis* **1987**, 823.

(21) (a) Moderhack, D.; Goos, K.-H.; Preu, L. *Chem. Ber.* **1990**, *123*, 1575. (b) Garbrecht, W. L.; Herbst, R. M. *J. Org. Chem.* **1953**, *18*, 1014. (c) Herbst, R. M.; Roberts, C. W.; Harvill, E. J. *J. Org. Chem.* **1951**, *16*, 139. (d) Marchalin, M.; Martvon, A. *Collect. Czech. Chem. Commun.* **1980**, *45*, 2329.

(22) Ried, W.; Erle, H.-E. *Liebigs Ann. Chem.* **1982**, 201.

(23) (a) Finnegan, W. G.; Henry, R. A.; Lieber, E. *J. Org. Chem.* **1953**, *18*, 779. (b) Jensen, K. A.; Holm, A.; Rachlin, S. *Acta Chem. Scand.* **1966**, *20*, 2795.

SCHEME 1

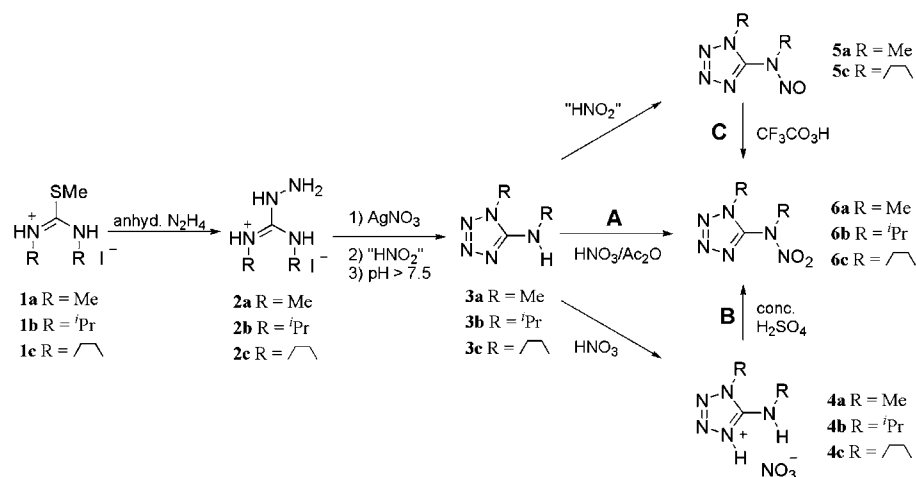


TABLE 1. Synthesis of the 5-Aminotetrazole Derivatives **3a–c**, **5a**, **5c**, and **6a–c**

entry	compd	yield [%]	method			mp (lit. mp) [°C]
			A	B	C	
1	3a	82 ^a				175.0–175.5
2	3b	71 ^a				163.5–164.0
3	3c	75 ^a				175.0–175.5
4	5a	84 ^b				46.0–47.0 (46–47 ^e)
6	5c	94 ^b				110.0–110.5 (–)
7	6a	64 ^c	81 (75 ^f) ^b	82 ^d		58.0–58.5 (58 ^e)
8	6b	66 ^c	75 ^b			56.0–57.0 (–)
9	6c	68 ^c (75 ^e)	64 ^b	80 ^d		150.0 dec (160 ^e)

^a Based on the corresponding thiourea derivative. ^b Based on the corresponding 5-aminotetrazoles. ^c Based on the corresponding nitrate (Supporting Information). ^d Based on the corresponding 5-nitrosoaminotetrazole. ^e See ref 11a. ^f See ref 11b.

known procedures from the substituted *S*-methyl-isothiuronium hydriodides (**1a–c**), which were first converted to the corresponding guanidinium derivatives (**2a–c**) with anhydrous hydrazine. Compounds **2a–c** were then reacted with nitrous acid followed by a base workup to yield the 5-aminotetrazoles in good overall yields (**3a** (82%), **3b** (71%), **3c** (75%), Scheme 1). A detailed experimental description of this reaction sequence can be found in Supporting Information.

The 5-aminotetrazoles (**3a–c**) are converted to the corresponding nitraminotetrazoles (**6a–c**) using the nitration system acetic anhydride/nitric acid (Scheme 1, A) or via the corresponding nitrates (**4a–c**), as described by Garrison and Herbst¹⁴ for the nitration of **3a** (Scheme 1, B). The obtained yield for **6c** by the direct nitration differs from that mentioned in ref 11a by 7%, and in the case of the methyl-substituted derivative (**6a**) a higher yield was obtained compared to that of Garrison and Herbst (Table 1).¹⁴ It is known from literature that peroxytrifluoroacetic acid (CF₃CO₃H) has been found to be a unique reagent for the oxidation of nitrosamines,²⁴ and to our knowledge this reagent has never been used for the oxidation of nitrosaminotetrazoles. The corresponding nitrosoamines were obtained according to known procedures only in the case of **5a** and **5c**. For **5b** no conversion to the corresponding nitramine **6b** was observed.^{11b} In the case of **3b** the reaction with nitrous acid resulted in the formation of a complex mixture of products from which it was not possible to isolate **5b**. Compounds **5a** and **5c**

were converted to **6a** and **6c** by CF₃CO₃H in DCM in excellent yields (82% and 80%, respectively, Scheme 1, C).

Molecular Structures. Selected data on the molecular geometry of the compounds **5a,c**, **6a–c** and the corresponding 5-aminotetrazoles **3a,c** are given in Table S1 (Supporting Information). The molecular structures of **3a,c**, **5a,c**, and **6a–c** in the crystal are shown in Figures 2, 3 and 4, respectively. Compounds **3a** and **6a** (Figure 2) crystallize in the orthorhombic space group *Pbca* with eight formula units in the unit cell; **3c** (Figure 3) and **6b** (Figure 4) in the monoclinic space group *P2₁/n* with four formula units in the unit cell.

In the case of **5a** (Figure 2), **5c** (Figure 3), and **6a** (Figure 2) the structures were solved in the monoclinic space group *P2₁/c* with four units in the unit cell. Comparing all investigated compounds with respect to the tetrazole moiety and the exocyclic atoms N5 and C2 (i.e., the lengths of the N–C and N–N bonds as well as the corresponding bond angles) the tetrazole rings are approximately planar within the limits of accuracy (maximal deviation is 0.060(1) Å for **3c** and 0.042(2) Å for **6a** from this plane; Table S3, Supporting Information). The geometrical parameters found compare well to those observed for other tetrazole derivatives.²⁵ The interatomic distances in the tetrazole rings are not equal, ranging from 1.284(3) to 1.384(2) Å. In the case of the aminotetrazoles **3a** and **3c**, the amino groups are planar in accord with a sp² hybridization of the nitrogen atom. The angle sums around N5 are 356° (**3a**) and 351° (**3c**), respectively (Table S2; Supporting Information). Moreover, the C1–N5 bond lengths in **3a** and **3c** compared to those in the nitrosamines and nitramines are closer to those typical for C=N double bonds. In the case of the substitution of the proton by a nitroso or nitro group, an elongation of the C1–N5 bond is found, with a maximum of 1.397(2) Å for **6b**. Depending on the nature of the substituent at N5, different features in the molecular structures of the investigated compounds were observed.

The formal exchange of the proton in **3a** and **3c** by a nitroso group leads to the *N*-nitrosamines **5a** (Figure 2) and **5c** (Figure 3). The nitrosamine moiety in **5a** and **5c** lies almost in the plane of the tetrazole ring; the dihedral angle between the tetrazole

(24) Shustov, G. V.; Rauk, A. *J. Org. Chem.* **1995**, *60*, 5891.

(25) (a) Lyakhov, A. S.; Vorobiov, A. N.; Gaponik, P. N.; Ivashkevich, L. S.; Matulis, V. E.; Ivashkevich, O. A. *Acta Cryst.* **2003**, *C59*, o690. (b) Lyakhov, A. S.; Voitekovich, S. V.; Gaponik, P. N.; Ivashkevich, L. S. *Acta Cryst.* **2004**, *C60*, o293. (c) Ohno, Y.; Akutsu, Y.; Arai, M.; Tamura, M.; Matsunaga, T. *Acta Cryst.* **2004**, *C60*, 1014.

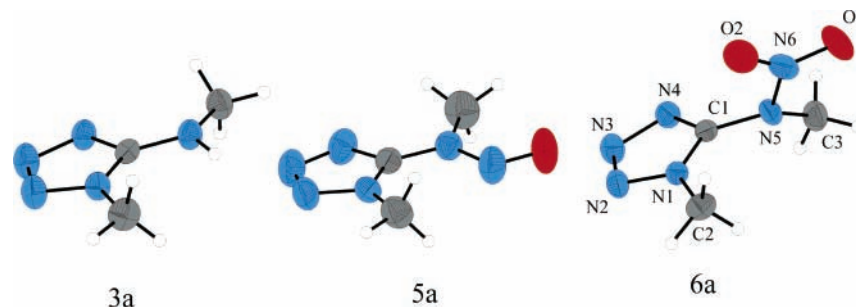


FIGURE 2. Molecular structures and labeling scheme for **3a**, **5a**, and **6a** (ORTEP plot, thermal ellipsoids represent 50% probability).

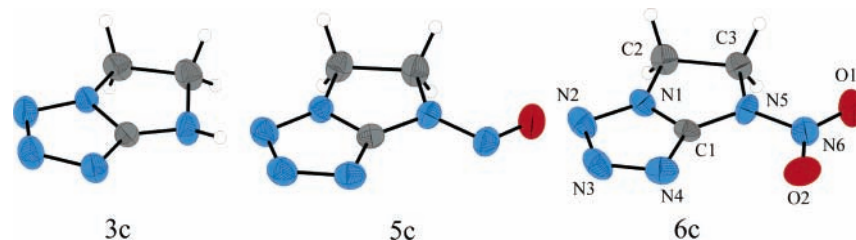


FIGURE 3. Molecular structures and labeling scheme for **3c**, **5c**, and **6c** (ORTEP plot, thermal ellipsoids represent 50% probability).

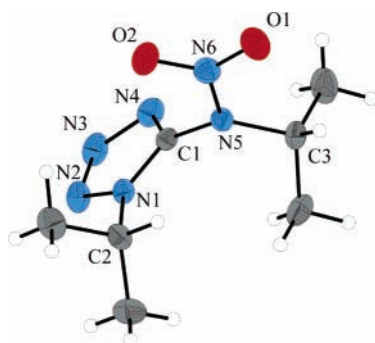


FIGURE 4. Molecular structure and labeling scheme **6b** (ORTEP plot, thermal ellipsoids represent 50% probability).

plane and the $-N(NO)-$ plane is 3.8° in the case of **5a** and 7.2° in the case of **5c**. The relevant torsion angles are given in Table S2 (Supporting Information). It is known that nitroso groups exhibit orientational disorder in the solid state,²⁶ which often leads to situations in which both isomers, *Z* (cisoid with respect to C–N) and *E* (transoid with respect to C–N), occupy the same site in the crystal. However, the crystal structure of **3a** and **3c** reveals that the *N*-nitrosamine moiety is ordered and adopts the *E* conformation (Figures 2 and 4). No residual electron density peaks were found in the nearest vicinity of this group in both compounds, indicating that the crystal indeed consists solely of the *E* rotamere. Compared to reported values of *N*-methyl-*N*-nitrosoanilines, the observed bond lengths differ dramatically.²⁷ The bond distance C1–N5 in **5a** (1.385(2) Å) and **5c** (1.378(2) Å) is much shorter than corresponding C–N bonds in nitrosoanilines, which are typically longer than 1.43 Å. The N5–N6 bond is much longer (1.335(3) Å (**5a**) and

1.331(2) Å (**5c**) vs ~ 1.30 Å in *N*-methyl-*N*-nitrosoanilines) and the N6–O1 bond (1.227(2) (**5a**) and 1.223(2) (**5c**) Å) was found to be shortened by ~ 0.04 Å with respect to the corresponding bond length in nitrosoanilines. An explanation for this might be the better π -conjugation of the tetrazole moiety with the lone pair at the N5 compared to anilines, which results in a shortening of the C1–N5 bond together with an elongation of the N5–N6 bond (see below, NBO analysis). Bond lengths and angles of the tetrazole fragments for both compounds agree well with the geometry of similar molecules bearing substituents inducing sp^2 hybridization at the amino nitrogen atom N5.

Selected bond length and bond angles of **6a** (Figure 2, left), **6b** (Figure 4), and **6c** (Figure 3, left) are contained in Table S2 (Supporting Information). For all three compounds the tetrazole ring and the arrangement around the nitrogen atoms of the nitramine moiety is planar within the limits of accuracy of the structure determination. The bond length and angles of the nitramine group for **6a–c** are comparable to those already reported.²⁸ In all three cases the lone pair on N5 is stereochemically inactive, which makes the bond angles about N5 essentially trigonal planar (angle sums around N5: $352.6(2)^\circ$ (**6a**), $358.1(1)^\circ$ (**6b**), and $359.4(3)^\circ$ (**6c**), respectively). This is found to be typical for unstrained nitramine units.²⁸ In the case of **6c** some differences with respect to certain structural parameters are observed. Compared to the nitramine moiety in **6a** and **6b**, which is almost perpendicular to the plane of the tetrazole ring (torsion angle N1–C1–N5–N6, $-78.5(2)^\circ$ (**6a**) and $-90.3(2)^\circ$ (**6b**)), the nitramine moiety in **6c** lies in the same plane as the tetrazole ring (N1–C1–N5–N6, $-176.28(1)^\circ$), indicating a possible interaction between the π -system of the tetrazole ring and the nitramine unit. The π -electron delocalization in **6c** is reflected, e.g., in the bond distance C1–N5 (1.370(4) Å), which was found to be shortened by ~ 0.03 Å compared to **6a** (1.391(3) Å) and **6b** (1.397(2) Å). This is also supported by the results of an NBO analysis (see below). In accordance with that the N5–N6 bond was found to be unusually shortened in the case of **6c**

(26) (a) Gdaniec, M.; Milewska, M. J.; Połonoński, T. *J. Org. Chem.* **1995**, *60*, 7411. (b) Olszewska, T.; Milewska, M. J.; Gdaniec, M.; Małuszyńska, H.; Połonoński, T. *J. Org. Chem.* **2001**, *66*, 501.

(27) (a) Ohwada, T.; Miura, M.; Tamaka, H.; Sakamoto, S.; Yamaguchi, K.; Ikeda, H.; Inagaki, S. *J. Am. Chem. Soc.* **2001**, *133*, 10164. (b) Chakrabarti, P.; Venkatesan, K. *J. Chem. Soc., Perkin Trans. 1* **1981**, 206. (c) Constable, A. G.; McDonald, W. S.; Shaw, B. L. *J. Chem. Soc., Dalton Trans.* **1980**, 2282.

(28) (a) Filhohl, A.; Bravic, G.; Rey-Lafon, M.; Thomas, M. *Acta Cryst.* **1980**, *B36*, 575. (b) Ejsmont, K.; Kyzioł, J.; Daszkiewicz, Z.; Bujak, M. *Acta Cryst.* **1998**, *C54*, 672.

(1.354(4) Å) compared to **6a** (1.390(3) Å) and **6b** (1.376(2) Å). The differences of the nonbridged structures such as **6a** and **6b** compared to **6c** can be best explained by repulsive interaction of the sp^2 -type lone pair at N4 and the electron density localized at O2 of the nitro groups. This interaction leads to the orthogonal structure in **6a** and **6b** since the O2 atom of the nitro group tries to be as distant as possible from N4. Consequently a large N4–O2 distance is found in **6a** (3.510(1) Å) and **6b** (3.329(1) Å), compared to a fairly short distance in **6c** (2.880(2) Å).

Since densities of explosives are important for predicting explosive properties, a semiempirical computer program invented by Willer et al., China Lake, was used to calculate the densities of compounds **6a–c**. The predicted densities are 1.53 (**6a**), 1.27 (**6b**), and 1.71 (**6c**) g cm⁻³. The calculated data agrees remarkably well with the densities measured by X-ray crystallography (Table S1, 1.522, 1.305 and 1.690 g cm⁻³, respectively; Supporting Information) and also illustrate that the cyclic compounds shows higher densities than the acyclic compounds.⁵³

NBO Analysis. A striking feature of the structure of all investigated tetrazolyl substituted nitroso- and nitramines is the

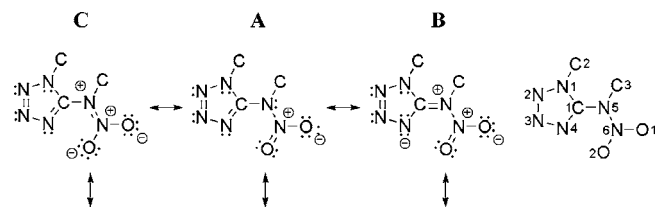


FIGURE 5. Lewis representation of the donor–acceptor interaction of p-LP(N5) with $\pi^*(C1-N4)$ (B) and $\pi^*(O1-N6)$ (C), respectively.

TABLE 2. Summary of the NBO Analysis of **5a,c** and **6a–c** (p-LP(N5) $\rightarrow \sigma/\pi^*(XY)$ Donor–Acceptor Interactions in kcal mol⁻¹)^a

	5a	5c	6a	6b	6c
p-LP(N5) $\rightarrow \pi^*(C1-N4)$	47.9	48.5	7.7	0.8	47.4
p-LP(N5) $\rightarrow \sigma^*(O1-N6)$	50.4	54.8	40.1	43.6	45.2
Σ_{NO/NO_2}^a	54.2	57.9	51.2	52.0	52.0
Σ_{ring}^a	51.2	50.9	28.3	22.9	50.3

^a The experimental data have been used in the NBO algorithm.

almost planar environment of the nitrogen atom N5 (angle sums around N5 ranging from 352.6(2)° to 360.0(2)°, Table S2; Supporting Information). As shown by NBO analysis,²⁹ in all investigated species the lone pair at the nitrogen atom N5 is localized in a pure p-type atomic orbital. As a consequence the p-type lone pair at the nitrogen atom N5 (notation: p-LP(N5)) can be further delocalized resulting in intramolecular interactions (noncovalent effects). The best Lewis representation according to NBO is given in Figure 5 (A) and displays two double bonds between C1–N4 and N2–N3 of the tetrazolyl ring.

This finding is also supported by the calculated Wiberg bond indices (Table S4; Supporting Information). Investigation of the noncovalent effects reveals two main possibilities for delocal-

(44) (a) Gropen, O.; Skancke, P. N. *Acta Chem. Scand.* **1971**, 25, 1241. (b) Gdaniec, M.; Milewska, M. J.; Polonski, T. *J. Org. Chem.* **1995**, 60, 7411.

(45) (a) Harris, R. K.; Pryce-Jones, T.; Swinbourne, F. J. *J. Chem. Soc., Perkin Trans. 2* **1980**, 476. (b) *N-Nitrosoindoline* and *N-methyl-N-phenylnitrosamine* exist as a single conformational isomer; see: Looney, C. E.; Phillips, W. D.; Reilly, E. L. *J. Am. Chem. Soc.* **1957**, 79, 6136. The rotational barrier of an aromatic *N-nitrosamine*, *N-nitrosodiphenylamine*, was reported to be 19.1 kcal/mol by Forlani et al.: Forlani, L.; Lunazzi, L.; Macciantelli, D.; Minguzzi, B. *Tetrahedron Lett.* **1979**, 1451.

(46) Kintzinger, J. P.; Lehn, J. M.; Williams, R. L. *Mol. Phys.* **1969**, 17 (1), 137.

(47) (a) Habibollahzadeh, D.; Murray, J. S.; Redfern, P. S.; Politzer, P. *J. Phys. Chem.* **1991**, 95, 7702. (b) Habibollahzadeh, D.; Murray, J. S.; Grice, M. E.; Politzer, P. *Int. J. Quant. Chem.* **1993**, 45, 15.

(48) *ICT-Thermodynamic Code*, Version 1.0; Fraunhofer-Institut für Chemische Technologie (ICT): Pfinztal/Berghausen, Germany, 1988–2000.

(49) Kistiakowsky, G. B.; Romeyn, H. Jr.; Ruhoff, J. R.; Smith, A. H.; Vaughan, W. E. *J. Am. Chem. Soc.* **1935**, 56, 1112.

(50) (a) Kamlet, M. J.; Jacobs, S. J. *J. Chem. Phys.* **1968**, 48, 23. (b) Kamlet, M. J.; Ablard, J. E. *J. Chem. Phys.* **1968**, 48, 36. (c) Kamlet, M. J.; Dickinson, C. J. *J. Chem. Phys.* **1968**, 48, 43. (d) Eremenko, L. T.; Nesterenko, D. A. *Chem. Phys. Rep.* **1997**, 16, 1675. (e) Astakhov, A. M.; Stepanov, R. S.; Babushkin, A. Y. *Combust. Explosives. Shock Waves* **1998**, 34, 85 (Engl. Transl.).

(51) With $K = 15.58$, ρ [g cm⁻³]; $\varphi = N\sqrt{M(-\Delta_E H)}$; N = moles of gases per g of explosives; M = average molar mass of formed gases; $\Delta_E H$ = calculated enthalpy of detonation (in cal g⁻¹); $A = 1.01$; $B = 1.30$.

(52) Lothrop W. C.; Handrick G. R. *Chem. Rev.* **1949**, 44, 419.

(53) Willer, R. L.; Chafin, A. P.; Doyle, J. P. *Energy-A Computer Program for Calculated the Density, Detonation Velocity, and Detonation Pressure of Proposed Energetic Materials*; NWC Technical Memorandum 5144, August 1983.

(54) Mader, C. L. Report LA-2900, Los Alamos Scientific Laboratory; *Detonation Properties of Condensed Explosives Computed Using the Becker-Kistiakowsky-Wilson Equation of State*; Los Alamos, NM, 1963.

(29) (a) Reed, A. E.; Curtiss, L. A.; Weinhold, F. *Chem. Rev.* **1988**, 88, 899. (b) Reed, A. E.; Weinstock R. B.; Weinhold, F. *J. Chem. Phys.* **1985**, 83, 735.

(30) (a) Claramunt, R. M.; Sanz, D.; López, C.; Jiménez J. A.; Jimeno, M. L.; Elguero, J.; Fruchier, A. *Magn. Reson. Chem.* **1997**, 35, 35. (b) Koren, A. O.; Gaponik, P. N. *Khim. Geterosikl. Soedin.* **1990**, 1643. (c) Begtrup, M.; Elguero, J.; Faure, R.; Camps, P.; Estopa, C.; Ilavsky, D.; Fruchier, A.; Marzin, C.; Mendoza, J. de *Magn. Reson. Chem.* **1988**, 26, 134.

(31) Nelson, J. H.; Takach, N. E.; Henry, R. A.; Moore, D. W.; Tolles W. M.; Gray, G. A. *Magn. Reson. Chem.* **1986**, 24, 984 1986 and references therein.

(32) (a) Kricheldorf, H. R. *Org. Magn. Reson.* **1980**, 13, 52. (b) Sogn, J. A.; Gibbon, Randall, E. W. *Biochemistry* **1973**, 12, 2100.

(33) Frisch, M. J.; Trucks, G. W.; Schlegel, H. B.; Scuseria, G. E.; Robb, M. A.; Cheeseman, J. R.; Zakrzewski, V. G.; Montgomery, J. A.; Stratmann, Jr., R. E.; Burant, J. C.; Dapprich, S.; Millam, J. M.; Daniels, A. D.; Kudin, K. N.; Strain, M. C.; Farkas, O.; Tomasi, J.; Barone, V.; Cossi, M.; Cammi, R.; Mennucci, B.; Pomelli, C.; Adamo, C.; Clifford, S.; Ochterski, J.; Petersson, G. A.; Ayala, P. Y.; Cui, Q.; Morokuma, K.; Malick, D. K.; Rabuck, A. D.; Raghavachari, K.; Foresman, J. B.; Cioslowski, J.; Ortiz, J. V.; Stefanov, B. B.; Liu, G.; Liashenko, A.; Piskorz, P.; Komaromi, I.; Gomperts, R.; Martin, R. L.; Fox, D. J.; Keith, T.; Al-Laham, M. A.; Peng, C. Y.; Nanayakkara, A.; Gonzalez, C.; Challacombe, M.; Gill, P. M. W.; Johnson, B.; Chen, W.; Wong, M. W.; Andres, J. L.; Gonzalez, C.; Head-Gordon, M.; Replogle, E. S.; Pople, J. A. *Gaussian 98*, Revision A.6; Gaussian, Inc.: Pittsburgh, PA, 1998.

(34) Wiberg, K. B.; Raben, P. R. *J. Comput. Chem.* **1993**, 14, 1504.

(35) (a) Bonnett, R.; Hollyhead, R.; Johnson, B. L.; Randall, E. W. *J. Chem. Soc.* **1964**, 86, 5564. (b) Gouesnard, J. P.; Martin, G. *J. Org. Magn. Reson.* **1979**, 12, 263. (c) Willer, R. L.; Lowe-Ma, C. K.; Moore, D. W. *J. Org. Chem.* **1984**, 49, 1481. (d) Witanowski, M.; Biedrzycka, Z.; Sicinska, W.; Grabowski, Z. *J. Magn. Reson.* **2003**, 164, 212.

(36) Gouesnard, J. P.; Martin, G. *J. Org. Magn. Reson.* **1979**, 12, 263.

(37) Kupper, R.; Hilton, B. D.; Kroeger-Koepke, M. B.; Koepke, S. R.; Michejda, C. J. *J. Org. Chem.* **1984**, 49, 3781.

(38) Witanowski, M.; Stefaniak, L.; Webb, G. A. *Annu. Rep. NMR Spectrosc.* **1993**, 25.

(39) Witanowski, M.; Biedrzycka, Z.; Sicinska, W.; Grabowski, Z. *J. Mol. Struct.* **2002**, 602–603, 199.

(40) Daszkiewicz, Z.; Nowakowska, E. M.; Preźdo, W. W.; Kyzioł, J. B. *Pol. J. Chem.* **1995**, 69, 1437.

(41) Lunazzi, L.; Cerioni, G.; Ingold, K. U. *J. Am. Chem. Soc.* **1976**, 98, 7484.

(42) Freeman, J. P.; Graham, W. H. *J. Am. Chem. Soc.* **1967**, 89, 1761.

(43) (a) Loeppky, R. N.; Michejda, C. J. *N-Nitrosamines and Related N-Nitroso Compounds*; ACS Symposium Series 553; American Chemical Society: Washington, DC, 1994. (b) Oh, S. M. N. Y. F.; Williams, D. L. *H. J. Chem. Soc., Perkin Trans. 2* **1989**, 755. (c) Castro, A.; Leis, J. R.; Pena, M. E. *J. Chem. Soc., Perkin Trans. 2* **1989**, 1861. (d) Galtress, C. L.; Morrow, P. R.; Nag, S.; Smalley, T. L.; Tschantz, M. F.; Vaughn, J. S.; Wichems, D. N.; Ziglar, S. K.; Fishbein, J. C. *J. Am. Chem. Soc.* **1992**, 114 1406. (e) Santala, T.; Fishbein, J. C. *J. Am. Chem. Soc.* **1992**, 114, 8852.

TABLE 3. ^{15}N and ^{13}C NMR Chemical Shifts (ppm) and $^{15}\text{N},^1\text{H}$ Coupling Constants (J , Hz) of the Compounds Studied

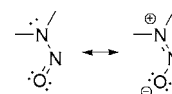
compd	N-1	N-2	N-3	N-4	N-5	X(N-6)	C-1
1 3a^a	-186.8 $^2J(\text{N1CH}_3) = 1.5$	-21.8 $^3J(\text{N2CH}_3) = 1.5$	1.8	-94.9 $^3J(\text{N4CH}_3) = 2.4$	-341.3 $^1J(\text{NH}) = 91.5$	(H)	155.7 ^b
2 3b^a	-164.6 $^2J(\text{N1CH}) = 2.6$	-28.8 $^3J(\text{N2CH}) = 2.2$	2.5	-94.7	-312.5 $^1J(\text{NH}) = 86.8$	(H)	153.5 ^b
3 3c^a	-163.3	-29.2 $^3J(\text{N2CH}_2) = 1.8$	21.0	-104.1 $^3J(\text{N4CH}_2) = 2.2$	-349.2 $^1J(\text{NH}) = 89.3$	(H)	165.8 ^a
4 5a^a	-168.0 $^2J(\text{N1CH}_3) = 2.0$	-9.1 $^3J(\text{N2CH}_3) = 1.7$	4.7	-72.8	-139.7 $^2J(\text{N5CH}_3) = 1.5$	172.7 (NO) ^c	153.3 ^b
5 5c^a	-153.5 $^2J(\text{N1CH}_2) = 1.9$	-23.5	24.9	-92.8	-144.6	167.4 (NO)	158.3 ^b
6 6a^a	-153.2 $^2J(\text{N1CH}_3) = 1.3$	-5.9	10.2	-58.9 $^3J(\text{N4CH}_3) = 2.2$	-219.6	-34.9 (NO ₂)	147.8 ^b
7 6b^a	-129.2 $^2J(\text{N1CH}) = 2.2$	-10.1 $^3J(\text{N2CH}) = 2.1$	13.3	-56.5	-202.2	-36.5 (NO ₂)	147.0 ^b
8 6c^a	-156.8 $^2J(\text{N1CH}_2) = 1.1$	-24.5	26.1	-83.2	-203.5	-42.0 (NO ₂)	158.6 ^b

^a d_6 -DMSO. ^b d_6 -Acetone. All shifts are given with respect to CH_3NO_2 (^{15}N) and TMS (^{13}C) as external standard; in the case of ^{15}N NMR negative shifts are upfield from CH_3NO_2 . ^c Coupling of protons α to the nitroso group to the nitroso nitrogen atom and are less than 1.0 Hz, for **5a** ($^3J(^{15}\text{N}-\text{H}) = 0.9$ Hz) – **5c** ($^3J(^{15}\text{N}-\text{H}) = 0.8$ Hz);

ization: into the tetrazolyl ring (B) or into the NO or NO₂ group (C). In case of the planar systems (**5a**, **5c**, **6c**) there are two significant interactions of the nitrogen lone pair (p-LP(N5)) with the two unoccupied, localized antibonding $\pi^*(\text{C1}-\text{N4})$ (B) and $\pi^*(\text{O1}-\text{N6})$ (C) orbitals, which is described by the resonance between the Lewis representations A, B, and C (Figure 5, Table 2). Moreover, delocalization into the NO (**5a**, **5c**) and NO₂ group (**6c**) is always slightly favored over the ring delocalization as indicated by the sum of the intramolecular donor–acceptor energies (Table 2, e.g., in **5a** $\Sigma_{\text{NO}}(54.2 \text{ kcal mol}^{-1}) > \Sigma_{\text{ring}}(51.2 \text{ kcal mol}^{-1})$).

For the two nonplanar species (**6a** and **6b**) the sum of the intramolecular donor–acceptor energies into the tetrazole moiety is as expected much smaller (Table 2, e.g., in **6a** $\Sigma_{\text{NO}_2}(51.2 \text{ kcal mol}^{-1}) > \Sigma_{\text{ring}}(28.3 \text{ kcal mol}^{-1})$). A comparison of the planar structures of **5a** and **5c** shows in the case of **5c** an unfavorable charge distribution. This is displayed by the electrostatic potential (ESP) mapped on the electronic density surface (Figure S2, Supporting Information) where a negatively charged tetrazole ring system is located next to the negatively charged nitroso group. In the case of **5a**, because of the different arrangement of the nitramine moiety, which is rotated by 180° compared to **5c**, such a repulsive interaction is not observed (Figure S3; Supporting Information). Therefore we can conclude that the significant interaction of the nitrogen lone pair (p-LP(N5)) with the two unoccupied, localized antibonding $\pi^*(\text{C1}-\text{N4})$ (B) and $\pi^*(\text{O1}-\text{N6})$ (C) orbitals, which describes the resonance between the Lewis representations A–C, is the driving force for the planarization of these systems. Interestingly, by oxidation of the nitroso group to the nitro group (**6a** and **6b**) these nonbridged structures are no longer planar since the lone pair on N4 and the electron density localized on the corresponding oxygen atom try to be as distant as possible from each other (Mulliken and NBO charges on N4 and O2; Table S5; Supporting Information). This situation is also nicely displayed by the corresponding ESPs mapped onto the electron density surface (Figure S4–6; Supporting Information). In the case of **6c**, from the electrostatic point of view the bridging ethylene unit forces this molecule in the unfavorable coplanar structure.

^{15}N Chemical Shifts and $^1\text{H}-^{15}\text{N}$ Coupling Constants. The ^{15}N NMR shifts and the values of the $^{15}\text{N},^1\text{H}$ coupling constants are presented in Table 3. For all compounds the proton coupled as well as the proton decoupled NMR spectra (with full NOE)

**FIGURE 6.** Resonance in *N*-nitrosamines.

were recorded. The assignments are based on the analysis of the $^{15}\text{N},^1\text{H}$ NMR coupling patterns in the proton decoupled NMR spectra and, where necessary, on the comparison with literature data.³⁰ In previous reports the assignments were associated with the assumption that in tetrazoles N-1 and N-4 in general resonate at lower frequency whereas N-2 and N-3 resonate at higher frequency and that alkyl substitution results in a significant shift of the pyrrole-type nitrogen resonance to lower frequency.³¹ In accordance with this, we find that the ^{15}N NMR chemical shifts correlate well with the electron densities at the nitrogen atoms (see above) and together with the $^{15}\text{N},^1\text{H}$ NMR coupling patterns the assignment of the ^{15}N NMR signals to the nitrogen atoms of the tetrazole moiety was straightforward.

In the case of the aminotetrazoles **3a–c**, the signal of the nitrogen atom (N-5) of the amino substituent could be assigned on the basis of its chemical shift, well-separated from the ^{15}N NMR signals of the nitrogen atoms of the tetrazole moiety, as well as its splitting to a doublet in the proton coupled ^{15}N NMR spectrum. The observed values for the one bond coupling constant are typical for $^1J(^{15}\text{N},^1\text{H})$ of three-coordinate nitrogen and range from 86.8 to 91.5 Hz (Table 3).³² For all the compounds **3a–c**, **5a,c**, and **6a–c** it was found that the ^{15}N NMR chemical shifts of the nitrogen atoms of the tetrazole ring become more negative in the order $\text{N-3} < \text{N-2} < \text{N-4} < \text{N-1}$. A more detailed insight into the electron charge distribution throughout the investigated compounds can be obtained from hybrid density functional theory (B3LYP). The optimized (B3LYP/6-31G(d,p))³³ geometries of the compounds have been used to calculate the electron charge distribution. The results summarized in Table S5 (Mulliken and NBO charges, Supporting Information) predict a general shift of electron charge toward the nitrosamino (**5a** and **5c**) and nitramino (**6a–c**) group and simultaneously an extreme differentiation of electron density throughout the tetrazole moiety. From these results using the Mulliken populations the atoms of the tetrazole moiety show the highest electron density of the two coordinated nitrogen atoms at N4. In the case of N2 and N3 the Mulliken population

TABLE 4. Potential Energy Barriers^a (kcal mol⁻¹) for Rotation about the N–N Bond in **5a**, **5c**, **6a**, and **6c**

compd	theor level	<i>syn</i> rotation about N–N bond (<i>sp_ts</i>) ^a	<i>anti</i> rotation about N–N bond (<i>ap_ts</i>) ^a	compd	theoret level	rotation about N–N bond (<i>ts</i>) ^a
5a	B3LYP/6-31G(d,p)	21.4 (21.2)	25.2 (23.3)	6a	B3LYP/6-31G(d,p)	12.8 (11.0)
	B3LYP/6-311+G(3df,2p)	21.1	23.9		B3LYP/6-311+G(3df,2p)	10.8
5c	B3LYP/6-31G(d,p)	18.0 (18.0)	21.2 (21.3)	6c	B3LYP/6-31G(d,p)	9.2 (9.4)
	B3LYP/6-311+G(3df,2p)	17.3	21.3		B3LYP/6-311+G(3df,2p)	8.5

^a Uncorrected values in kcal mol⁻¹. Values in parentheses is the Gibbs free energy: ΔG^\ddagger (298 K; kcal mol⁻¹).

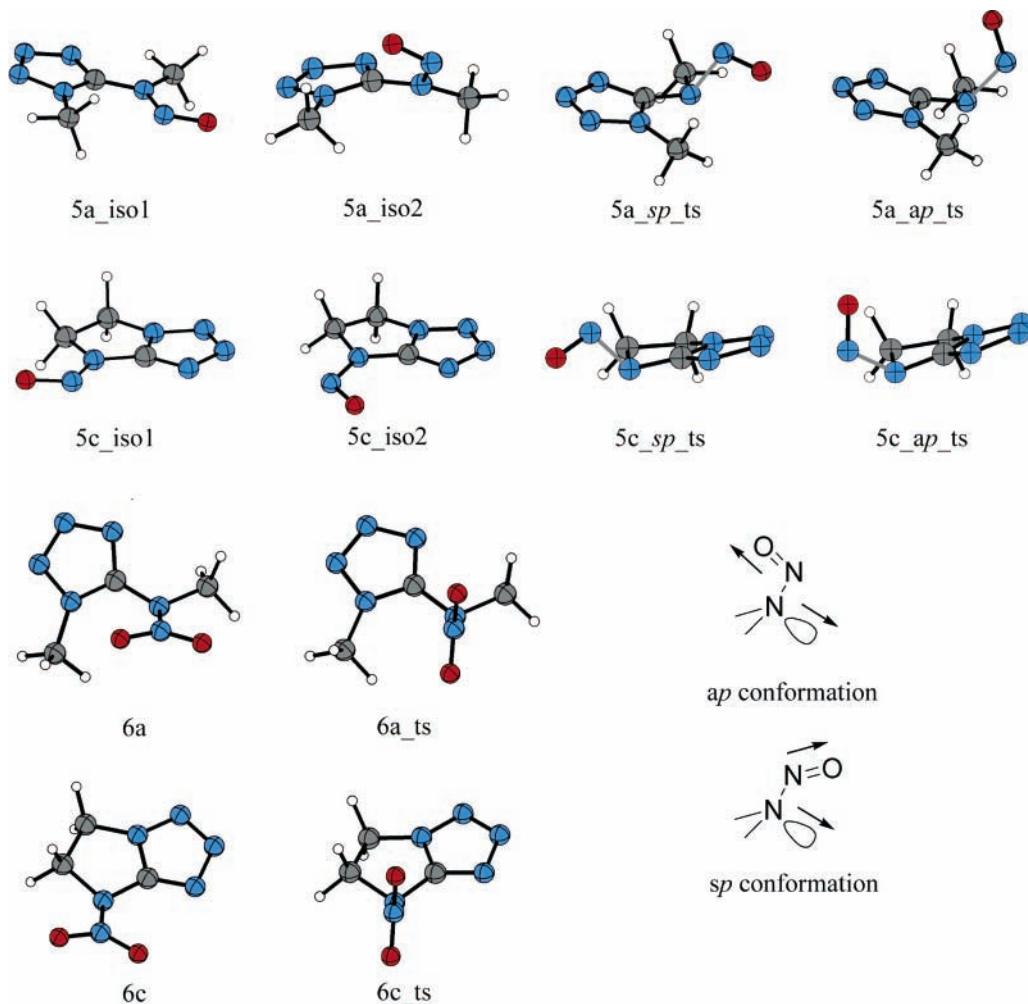


FIGURE 7. Optimized structures and transition states of *N*-nitrosaminotetrazoles **5a** and **5c** and *N*-nitraminotetrazoles **6a** and **6c**.

shows similar values, which are higher for N3 compared to N2. However, as the Mulliken population analyses are known to be basis set dependent, also the results from a natural population analysis were included. They also give similar values for N2 and N3, but now the values for N2 are slightly higher.³⁴ In addition, the nitrosamino as well the nitramino group carries an overall negative net charge, resulting in a substantial separation of charges between the tetrazole versus nitrosamino or nitramino moiety ($\Sigma q(\text{tetrazole}) = \sim +0.20\text{--}0.25e$ vs $\Sigma q(\text{nitrosamino/nitramino}) = \text{ca. } -0.20\text{--}0.25e$; Table S5; Supporting Information).

In accordance to the aminotetrazoles discussed previously, the ¹⁵N NMR signal of the amino nitrogen (N5) of the nitrosaminotetrazoles **5a** and **5c** also appears upfield from the nitromethane reference, while the signal of the nitroso nitrogen (N6) is found far at low field. In the case of the nitrosotetrazoles

5a and **5c**, the ¹⁵N chemical shift of the N=O nitrogen atom appears downfield relative to that of aliphatic nitrosamines in a range characteristic for aromatic nitrosamines, which also indicates extensive electron delocalization within the tetrazole moiety (NBO analyses).³⁵ Comparing the investigated nitrosamines (**5a** and **5c**) there is a remarkable upfield shift of 5.3 ppm from **5a** (172.7 ppm) to **5c** (167.4 ppm) which can be attributed to the different extent of crossconjugation into the tetrazole moiety, also observed in the NBO analysis.^{36,37}

The nitraminotetrazoles **6a–c** in a given solvent (*d*₆-DMSO) are good examples for the so-called β-effect of alkyl groups. It has already been observed that nitrogen magnetic shielding decreases significantly in the following sequence of alkyl substitution at nitrogen for a given group X (X = tetrazole moiety):³⁸ CH₃N(X) > RCH₂N(X) > R₂CHN(X) > R₃CN(X). R is an alkyl group, and X represents any atom or group of

atoms. This is called the β -effect as each step involves the introduction of a carbon atom at the β -position with respect to the nitrogen atom concerned and produces a deshielding effect $\Delta\sigma = 6\text{--}12$ ppm. In the present case, the replacement of the methyl group in **6a** by the isopropyl (**6b**) or ethylene bridge (**6c**), respectively, produces a β -effect and a concomitant deshielding of the amino nitrogen (N5), $\Delta\sigma =$ about 17 ppm, just within the range expected. In the case of the nitrogen atom (N6) of the nitro group the signals are observed at the expected region ($\delta = -20$ to -45 ppm).^{39,40} In the case of the **6c** a pronounced upfield shift for N6 (as well as N4) is observed (**6c** (N6, -42.0 ppm) vs, e.g., **6a** (N6, -34.9 ppm)) which can be attributed to the intramolecular donor–acceptor interaction of the π -system (see NBO analyses) of the tetrazole moiety with the nitramine unit (Table 2). For a detailed discussion of the ^1H , ^{13}C NMR data as well the dynamic behavior of compound **6b**, see Supporting Information.

N,N Rotational Barriers. The isomerization process that interchanges the alkyl groups, e.g., in Me_2NNO , requires roughly 23 kcal mol^{-1} .⁴¹ The mechanism is thought to involve rotation about the N–N bond rather than inversion of the nitroso nitrogen; calculations predict the latter to require activation energies that are four times as large as those of the rotation about the N–N bond.⁴² *N*-Nitroso compounds generally exhibit planar structures, because rotational barriers along the N–NO bond⁴³ are of similar magnitude compared to those of amides.⁴⁴ This can be understood in terms of a resonance structure (Figure 6), which displays partial double bond character of the N–N(O) bond, in a manner similar to the N–C(O) bond in amides.

A series of different types of nitrosamines have been investigated with respect to their rotational barriers. From these investigations, rotational barriers of monocyclic five-membered *N*-nitrosamines as well as other monocyclic *N*-nitrosamines are estimated to be larger than $20\text{--}21\text{ kcal mol}^{-1}$.⁴⁵

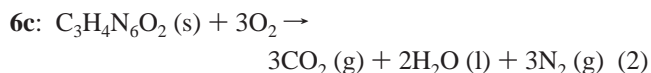
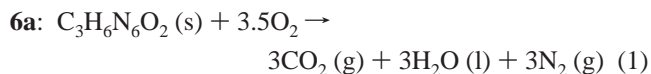
Rotational barriers with respect to the N–NO bonds were calculated with the Gaussian 98 program (Table 4).³³ The geometry optimizations were carried out at the B3LYP level of theory including the 6-31G(d,p) and 6-311+G(3df,2p) basis sets, using procedures implemented in the Gaussian molecular orbital packages. The calculated total energies for each calculated ground state structure as well as transition states (Figure 7) are given in Tables S6–8 (Supporting Information). Vibrational frequencies calculations were performed on all stationary points at the B3LYP level. Transition state structures were characterized by a single imaginary frequency, whereas the corresponding isomers (for **5a,c** iso1 and iso2; for **6a** and **6c** only one ground-state structure) had none. Two transitional rotational conformations of *N*-nitrosoamines were calculated for **5a** and **5c**, *s-cis* (*sp_ts*) and *s-trans* (*ap_ts*) conformations (NO bond syn-periplanar (*sp_ts*) or anti-periplanar (*ap_ts*) with respect to the nitrogen lone pair, Figure 7). In both cases, the *sp_ts* conformation was favored over the *ap_ts* conformation (Table 4).

This conformational preference can be interpreted in terms of repulsive interactions of the vicinal nitrogen lone pair of electrons of the amine and NO group in the *s-trans* rotated conformer. Rotational barriers about the N–NO bonds were evaluated on the basis of the most stable ground minimum structure of the nitrosamines **5a** and **5c**, and the values are shown in Table 4. The rotational barrier of the *N*-nitrosaminotetrazoles **5a** and **5c** was evaluated computationally to be $21.2\text{ kcal mol}^{-1}$ (**5a**) and $18.0\text{ kcal mol}^{-1}$ (**5c**) (B3LYP/6-31G(d,p)). These

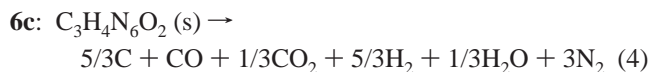
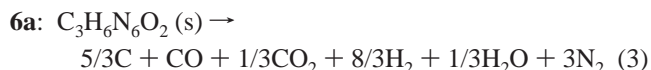
values compare well with those of the barriers of monocyclic nitrosamines.

In the case of the *N*-nitrosaminotetrazoles **6a** and **6c**, the corresponding rotational barriers about the N–NO₂ bonds were also evaluated on the basis of the most stable ground minimum structures (Figure 7), and the values are shown in Table 4. The barrier of internal rotation around the N–N bond in, e.g., the *N,N*-dimethylnitramine molecule, was determined experimentally to 9 kcal mol^{-1} ⁴⁶ and estimated theoretically to $4\text{--}13\text{ kcal mol}^{-1}$.⁴⁷ The rotation of the NO₂ group by 90° , i.e., perpendicular to the C1–N5–C3 plane, increases the N–N bond length and the arrangement of the C–N and N–N bonds around the amide nitrogen atom becomes tetrahedral.⁴⁶ In the case of **6a** and **6c** rotational barriers of comparable magnitude were obtained with values of 11.0 and 9.4 kcal mol^{-1} , respectively. Interestingly, the computed barriers apparently seem to correlate with the observed bond angles C1–N5–C3, indicating that the low rotational barrier of the N–NO as well as at the N–NO₂ bond of the investigated compounds is due to angle strain at the amino nitrogen atom (e.g., **5a** $119.9(2)^\circ$ vs **5c** $110.1(1)^\circ$ and **6a** $120.6(2)^\circ$ vs **6c** $110.0(3)^\circ$).

Thermochemistry. The heats of combustion for the compounds **6a** and **6c** were determined experimentally, and the molar enthalpies of formation were calculated from a designed Hess thermochemical cycle according to reactions 1 and 2. Typical experimental results (averaged over three measurements each) of the combustion energy at constant volume ($\Delta_c U$) for the compounds are given in Table 5. The standard molar enthalpy of combustion ($\Delta_c H^\circ$) was derived from $\Delta_c H^\circ = \Delta_c U + \Delta nRT$ ($\Delta n = \sum n_i$ (products, g) $- \sum n_i$ (reactants, g); $\sum n_i$ is the total molar amount of gases in products or reactants).



$$\Delta_f H_m^\circ = x\Delta_f H_m^\circ(\text{CO}_2, \text{g}) + y\Delta_f H_m^\circ(\text{H}_2\text{O}, \text{l}) - \Delta_c H_m^\circ$$



The enthalpies of detonation ($\Delta_E H_m^\circ$) for **6a** and **6c** were calculated with the ICT thermodynamic code.⁴⁸ To assess more quantitatively the expected detonation properties of **6a** and **6c**, the modified Kistiakowsky–Wilson Rule⁴⁹ (reactions 3 and 4, Ω lower than -40%) was used to calculate the expected detonation pressures (P) and detonation velocities (D) as well as the semiempirical equations suggested by Kamlet and Jacobs (eqs 5 and 6, Table 5).^{50,51}

The values thus obtained reach in the case of **6c** those of TNT with respect to the detonation pressure (22.0 GPa vs TNT,⁵⁴ $P = 20.6\text{ GPa}$) and those of nitroglycerin with respect to the detonation velocity (7181 m s^{-1} vs nitroglycerin,⁵⁵ $D = 7610\text{ m s}^{-1}$). Both compounds show a high gas yield, calculated

(55) Köhler, J.; Meyer, R. *Explosivstoffe*, 7. Aufl.; Wiley-VCH: Weinheim, 1991.

TABLE 5. Thermochemical Properties of 6a and 6c

	6a	6c
formula	C ₃ H ₆ N ₆ O ₂	C ₃ H ₄ N ₆ O ₂
molar mass	158.12	156.10
N [%]	53.2	53.8
Ω [%] ^a	-70.8	-61.5
-Δ _c U _m [cal/g] ^b	3119	3247
-Δ _c H _m ^o [kcal/mol] ^c	489.9	503.9
Δ _f H _m ^o [kcal/mol] ^d	+2.8	+85.2
-Δ _E H _m ^o [kcal/kg] ^e	549	1035
density [g cm ⁻³] ^f	1.522	1.690
density [g cm ⁻³] calcd ^g	1.53	1.71
P [GPa] ^h	14.3	22.0
D [m s ⁻¹] ^h	5988	7181
gas volume (25°C) [mL/g] ⁱ	1010	934

^a Oxygen balance; see ref 52. ^b Experimental combustion energy at constant volume. ^c Experimental molar enthalpy of combustion. ^d Molar enthalpy of formation. ^e Calculated molar enthalpy of detonation, ICT thermodynamic code; see ref 48. ^f From crystal structure determination. ^g Calculated; see ref 53. ^h Calculated from semiempirical equations suggested by Kamlet and Jacobs; see refs 50 and 51. ⁱ Assuming only gaseous products, ICT thermodynamic code; see ref 48.

with the ICT thermodynamic code.

$$P[10^8 \text{ Pa}] = K\rho^2\varphi \quad (5)$$

$$D[\text{mm } \mu\text{s}^{-1}] = A\varphi^{1/2}(1 + B\rho) \quad (6)$$

Conclusion

Since experimental data, crystallographic parameters, and rotational barriers of *N*-nitroso and *N*-nitraminotetrazole are rare in the literature, we investigated examples with low carbon and hydrogen content with respect to those parameters. A detailed discussion of the ¹⁵N NMR data and structural parameters was given, and the intriguing bond situation was discussed in terms of natural bond analysis (NBO). The NBO analysis indicated in the case of the nitrosotetrazoles **5a** and **5c** two significant interactions of the nitrogen lone pair (p-LP(N5)) with the two unoccupied, localized antibonding π*(C1-N4) and π*(O1-N6) orbitals. In the case of the nonbridged nitro derivatives **6a** and **6b** the interaction with the antibonding π*(C1-N4) is no longer observed as a result of the rotation of the tetrazole moiety out of the nitramine plane. As the nitroso group is somewhat related to the structural features of amides, the special conformational behavior of the *N*-nitrosaminotetrazoles **5a** and **5c** is characterized by calculated high rotational barriers. They are found in the range typical for aromatic *N*-nitrosamines and are almost double in magnitude compared to those of the corresponding nitro derivatives **6a** and **6c**. In the case of **6a** and **6c**, the heat of formation was determined experimentally with bomb calorimetry resulting in positive values for both compounds. The heat of explosion estimated semiempirically with the help of the thermochemical ICT code was used to calculate the gas yield, indicating in both cases high amounts of produced gases (1010 (**6a**) and 934 (**6c**) mL g⁻¹).

Experimental Section

CAUTION: Although aminotetrazoles are kinetically stable and in most cases are insensitive to electrostatic discharge, friction, and impact, they are nonetheless energetic materials and appropriate safety precautions should be taken, especially in the case of the *N*-nitrosamino- and the *N*-nitraminotetrazoles. Laboratories and personnel should be properly grounded and safety equipment such as Kevlar gloves, leather coat, face shield, and ear plugs are

necessary when compounds **6a** and **6c** are synthesized on a larger scale. **With respect to the dangers likely to be encountered on a scale-up, this should be carefully thought out and special precautions need to be applied.** Moreover, since *N*-nitrosamines are known to have strong carcinogenic and mutagenic properties, special care has to be taken when manipulating **5a** and **5c**.

The amino-1*H*-tetrazoles were prepared according to previously published procedures.¹⁰ A detailed description of the procedure for **2a-c**, **3a-c**, and the corresponding nitrates **4a-c** is contained in Supporting Information.

General Procedure for the Preparation of 5-Nitrosoaminotetrazoles 5a and 5c. The nitrosoamines **5a** and **5c** were prepared following published procedures.^{11b} To a cooled solution of the respective amino-1*H*-tetrazole (25 mmol) in 50 mL of 2 M HCl was slowly added a solution of sodium nitrite (1.73 g, 25 mmol) in 20 mL of water. During the addition the temperature was maintained between 0 and 5 °C. The resulting mixture was stirred at 5–10 °C for 30 min and then brought to pH 8 with anhydrous potassium carbonate. In the case of **5a**, the aqueous solution was extracted with DCM (3 × 100 mL), and the combined organic extracts washed with water (2 × 70 mL) and dried over MgSO₄. After removing the solvent in vacuo the yellow residue was recrystallized from water/EtOH, yielding light-sensitive pale-yellow plates (84%). In the case of **5c**, the crude product separated during the addition of the potassium carbonate. Recrystallization from water/EtOH yielded pale-yellow needles (94%).

1-Methyl-5-(methylnitrosoamino)-1*H*-tetrazole (5a). Mp 46–47 °C. $\tilde{\nu}$ (KBr) [cm⁻¹]: 3040 (vw, -CH₃), 2954 (vw, -CH₃), 1626 (w), 1576 (vs, $\tilde{\nu}_{\text{asym}}$ NO), 1512 (m), 1464 (m), 1446 (vs), 1455 (vs), 1415 (m), 1391 (m), 1318 (vw), 1277 (m, $\tilde{\nu}$ -N-N=N⁺), 1225 (s, $\tilde{\nu}_{\text{sym}}$ NO), 1208 (m, $\tilde{\nu}$ tetrazole), 1125 (s, $\tilde{\nu}$ tetrazole), 1097 (s, $\tilde{\nu}$ tetrazole), 1037 (w, $\tilde{\nu}$ tetrazole), 973 (m), 946 (s, $\tilde{\nu}$ -CH₃N-NO), 814 (s), 730 (m), 701 (s), 691 (m), 519 (w), 462 (vw). Raman (200 mW) $\tilde{\nu}$ [cm⁻¹]: 3041 (11), 2966 (25), 1580 (100, $\tilde{\nu}_{\text{asym}}$ NO), 1511 (48), 1456 (11), 1418 (6), 1393 (13), 1318 (7, $\tilde{\nu}$ -N-N=N-), 1278 (16, $\tilde{\nu}_{\text{sym}}$ NO₂), 1097 (7, $\tilde{\nu}$ tetrazole), 1041 (2, $\tilde{\nu}$ tetrazole), 947 (11, $\tilde{\nu}$ -CH₃N-NO), 815 (9), 731 (4), 702 (37), 521 (6), 464 (23), 286 (4), 357 (8), 326 (7), 231 (6), 199 (13). ¹H NMR (CDCl₃) δ: 3.58 (s, 3H, -CH₃), 4.21 (s, 3H, CH₃). ¹³C NMR (*d*₆-acetone) δ: 32.1 (CH₃), 37.4 (CH₃), 153.3 (C). ¹⁴N NMR (CDCl₃) δ: 170 (N-NO, Δν_{1/2} = 1101 Hz), -6 (N2, N3 Δν_{1/2} = 1009 Hz), -75 (N4, Δν_{1/2} = 550 Hz), -141 (-NMe-NO, Δν_{1/2} = 459 Hz), -173 (N1, Δν_{1/2} = 367 Hz); *m/z* (EI) 143 [(M + H⁺) (15)], 127 (36), 126 (10), 113 (12), 83 (5), 71 (4), 70 (5), 69 (8), 52 (5), 43 (100), 42 (5), 41 (11), 40 (8), 30 (10), 28 (12), 15 (25). C₃H₆N₆O (142.12): Calcd C, 25.4; H, 4.3; N, 59.1. Found: C, 25.5; H, 4.3; N, 59.5.

7-Nitroso-5,6-dihydro-7*H*-imidazol[1,2-*d*]tetrazole (5c). Mp 110–110.5 °C (decomp). $\tilde{\nu}$ (KBr)[cm⁻¹]: 3028 (vw, -CH₂), 1585 (vs, $\tilde{\nu}_{\text{asym}}$ NO), 1536 (m), 1473 (vs), 1455 (vs), 1430 (m), 1358 (ms, 1315 (w), 1280 (vw), 1264 (s, $\tilde{\nu}$ -N-N=N⁺), 1240 (s, $\tilde{\nu}_{\text{sym}}$ NO), 1192 (s, $\tilde{\nu}$ tetrazole), 1157 (vs, $\tilde{\nu}$ tetrazole), 961 (m, $\tilde{\nu}$ -CH₃N-NO), 803 (s), 763 (m), 726 (m), 687 (vw), 604 (w), 516 (vw), 367 (vw), 337 (vw). Raman (200 mW) $\tilde{\nu}$ [cm⁻¹]: 3028 (17), 2987 (20), 2961 (22), 1584 (100, $\tilde{\nu}_{\text{asym}}$ NO), 1538 (27), 1481 (22), 1468 (21), 1456 (37), 1357 (2), 1316 (13, $\tilde{\nu}$ -N-N=N-), 1263 (15, $\tilde{\nu}_{\text{sym}}$ NO₂), 1235 (8), 1206 (7, $\tilde{\nu}$ tetrazole), 1187 (6, $\tilde{\nu}$ tetrazole), 1158 (6, $\tilde{\nu}$ tetrazole), 1045 (14, $\tilde{\nu}$ tetrazole), 963 (5, $\tilde{\nu}$ tetrazole), 933 (5, $\tilde{\nu}$ -CH₃N-NO), 802 (4), 764 (31), 729 (3), 605 (21), 518 (32), 409 (23), 365 (8), 349 (16), 207 (19), 126 (8). ¹H NMR (*d*₆-DMSO) AA'BB'-spectrum (δ_A = 4.64, δ_B = 4.72, N = 31 Hz, CH₂). ¹³C NMR (*d*₆-acetone) δ: 43.0 (CH₂), 53.9 (CH₂), 158.3 (C); *m/z* (EI) 140 [(M⁺) (100)], 109 (5), 96 (25), 67 (9), 55 (60), 54 (27), 53 (44), 44 (5), 41 (5), 40 (7), 30 (51), 28 (90), 27 (15). C₃H₄N₆O (140.10): Calcd C, 25.7; H, 2.9; N, 60.0. Found: C, 25.6; H, 3.3; N, 59.7.

General Procedures for Preparation of 5-Nitraminotetrazoles 6a–c. Method A; 6a–c. The amino-1*H*-tetrazoles **3a–c** were transformed according known procedures (for details see Supporting Information) to the corresponding amino-1*H*-tetrazolium nitrates.¹⁴

The nitrate (20 mmol) was slowly added with stirring to cooled (ca. $-8\text{ }^{\circ}\text{C}$) concentrated sulfuric acid (4.5 mL). During the addition of the nitrate the temperature of the reaction mixture should not exceed $0\text{ }^{\circ}\text{C}$. After the addition the reaction mixture was stirred for further 10 min, quickly heated to $25\text{ }^{\circ}\text{C}$, and poured onto 30 g of ice. The white crystalline solid was separated by filtration and washed with water until it became acid free and was recrystallized from an appropriate (see below) solvent. A second crop of product was obtained by extracting the aqueous solution with Et_2O followed by the workup procedures described above. **Method B; 6a–c**. The method described in^{11a} was used. To cooled acetic anhydride (5 g; ice bath), 5 g of 100% nitric acid was added dropwise over 10 min. After 20 min, 25 mmol of the respective amino-1*H*-tetrazole was added in small portions over 10 min. The solution was stirred for further 20 min and then quenched on 25 g of crushed ice. The crude product was collected, washed until it became acid free, and recrystallized from an appropriate (see below) solvent. **Method C; 6a and 6c**. To a well stirred suspension of 0.41 mL (15 mmol) of 90% hydrogen peroxide in 10 mL of DCM (cooling with an ice-bath recommended) was added 2.60 mL (18 mmol) of trifluoroacetic anhydride in one portion. After 5 min the solution was allowed to warm to room temperature and 10 mmol of the corresponding nitrosamine in 5 mL of DCM was added dropwise over a 30-min period. During this addition an exothermic reaction occurred, which caused the solution to boil. After the addition was completed the mixture was heated under reflux for 1 h. The DCM solution was then washed with water ($3 \times 15\text{ mL}$) and dried over MgSO_4 . The solvent was removed by distillation under reduced pressure and the residue was recrystallized from an appropriate (see below) solvent.

1-Methyl-5-(methylnitramino)-1*H*-tetrazole (6a). Recrystallization from benzene/pentane. Mp $58\text{--}58.5\text{ }^{\circ}\text{C}$. $\tilde{\nu}(\text{KBr})$ [cm^{-1}]: 3038 (vw), 2961 (vw, $-\text{CH}_3$), 2925 (vw, $-\text{CH}_3$), 2854 (vw, $-\text{CH}_3$), 1576 (vs, $\tilde{\nu}_{\text{asym}} \text{NO}_2$), 1545 (m), 1487 (m), 1461 (m), 1430 (m), 1384 (w), 1314 (m, $\tilde{\nu} \text{-N-N=N}^+$), 1294 (s, $\tilde{\nu}_{\text{sym}} \text{NO}_2$), 1269 (m), 1214 (m, $\tilde{\nu}$ tetrazole), 1181 (m, $\tilde{\nu}$ tetrazole), 1127 (m, $\tilde{\nu}$ tetrazole), 1093 (m, $\tilde{\nu}$ tetrazole), 1049 (w), 989 (w), 949 (m, $\tilde{\nu} \text{-CH}_3\text{N-NO}_2$), 786 (m), 761 (m), 748 (w), 606 (m). Raman (200 mW) $\tilde{\nu}[\text{cm}^{-1}]$: 3038 (33), 3025 (34), 2962 (99), 2829 (9), 1551 (100, $\tilde{\nu}_{\text{asym}} \text{NO}_2$), 1488 (14), 1440 (25), 1418 (23), 1315 (27, $\tilde{\nu} \text{-N-N=N}^+$), 1291 (33, $\tilde{\nu}_{\text{sym}} \text{NO}_2$), 1270 (45, $\tilde{\nu}$ tetrazole), 1216 (26, $\tilde{\nu}$ tetrazole), 1153 (7, $\tilde{\nu}$ tetrazole), 1096 (15), 1051 (8), 991 (10), 951 (38, $\tilde{\nu} \text{-CH}_3\text{N-NO}_2$), 787 (70), 699 (63), 607 (32), 490 (40), 451 (27), 402 (22), 321 (15), 280 (24), 254 (20), 142 (74). $^1\text{H NMR}$ (d_6 -acetone) δ : 3.82 (s, 3H, CH_3), 4.10 (s, 3H, CH_3). $^{13}\text{C NMR}$ (d_6 -acetone) δ : 29.8 (CH_3), 35.7 (CH_3), 147.8 (C). $^{14}\text{N NMR}$ (d_6 -acetone) δ : 10 (N_2 , $\Delta\nu_{1/2} = 578\text{ Hz}$), -4 (N_3 , $\Delta\nu_{1/2} = 616\text{ Hz}$), -35 ($-\text{CH}_3\text{N-NO}_2$, $\Delta\nu_{1/2} = 23\text{ Hz}$), -58 (N_4 , $\Delta\nu_{1/2} = 374\text{ Hz}$), -155 (N_1 , $\Delta\nu_{1/2} = 181\text{ Hz}$), -219 ($-\text{CH}_3\text{N-NO}_2$, $\Delta\nu_{1/2} = 919\text{ Hz}$); m/z (CI, *i*-Buten) 159 [(M + H⁺) (100)]. $\text{C}_3\text{H}_6\text{N}_6\text{O}_2$ (158.12): Calcd C, 22.8; H, 3.8; N, 53.2. Found: C, 22.8; H, 3.9; N, 53.4.

1-Isopropyl-5-(isopropylnitramino)-1*H*-tetrazole (6b). Recrystallization from EtOH/water. Mp $56\text{--}57\text{ }^{\circ}\text{C}$. $\tilde{\nu}(\text{KBr})$ [cm^{-1}]: 2994 (vw, *i*-Pr), 2971 (vw, *i*-Pr), 2883 (vw, *i*-Pr), 2847 (vw, *i*-Pr), 1567 (vs, $\tilde{\nu}_{\text{asym}} \text{NO}_2$), 1469 (w), 1461 (w), 1448 (vw), 1426 (m), 1401 (vw), 1391 (w), 1385 (vw), 1375 (vw), 1350 (vw), 1321 (m, $\tilde{\nu} \text{-N-N=N}^+$), 1288 (s, $\tilde{\nu}_{\text{sym}} \text{NO}_2$), 1254 (vw), 1243 (vw), 1182 (w, $\tilde{\nu}$ tetrazole), 1164 (w, $\tilde{\nu}$ tetrazole), 1137 (vw, $\tilde{\nu}$ tetrazole), 1125 (m, $\tilde{\nu}$ tetrazole), 1091 (w, $\tilde{\nu}$ tetrazole), 1062 (w, $\tilde{\nu}$ tetrazole), 994 (vw), 970 (w, $\tilde{\nu} \text{-CH}_3\text{N-NO}_2$), 946 (vw), 934 (vw), 885 (vw), 792 (w), 760 (w), 736 (vw), 726 (vw), 668 (vw), 643 (vw), 589 (vw), 555. Raman (200 mW) $\tilde{\nu}[\text{cm}^{-1}]$: 2999 (100), 2990 (84), 2974 (80), 2946 (93), 2929 (69), 2875 (28), 2773 (6), 2733 (11), 1576 (12), 1522 (83, $\tilde{\nu}_{\text{asym}} \text{NO}_2$), 1457 (53), 1398 (29), 1322 (21), 1285 (40, $\tilde{\nu} \text{-N-N=N}^+$), 1253 (41, $\tilde{\nu}_{\text{sym}} \text{NO}_2$), 1183 (17, $\tilde{\nu}$ tetrazole), 1138 (29, $\tilde{\nu}$ tetrazole), 1092 (39, $\tilde{\nu}$ tetrazole), 1068 (29, $\tilde{\nu}$ tetrazole), 1048 (12), 994 (12), 948 (24, $\tilde{\nu} \text{-CH}_3\text{N-NO}_2$), 888 (45), 795 (60), 767 (12), 735 (10), 646 (42), 588 (19), 564 (19), 477 (41), 439 (49), 377 (17), 349 (34), 317 (24), 295 (24), 152 (84), 119 (44). *The*

compound shows in solution dynamic behavior. $^1\text{H NMR}$ (d_6 -acetone, $25\text{ }^{\circ}\text{C}$) δ : 1.31 (s, 6H, $\text{CH}(\text{CH}_3)_2$), 1.58 (d, 6H, $^3J\text{ }6.6\text{ Hz}$, $-\text{CH}(\text{CH}_3)_2$), 4.9 (septett, 1H, $^3J\text{ }6.6\text{ Hz}$, $-\text{CH}(\text{CH}_3)_2$), 5.07 (septett, 1H, $^3J\text{ }6.6\text{ Hz}$, $-\text{CH}(\text{CH}_3)_2$); (d_6 -acetone, $-65\text{ }^{\circ}\text{C}$) δ : 1.03 (d, 3H, $^3J\text{ }7.0\text{ Hz}$, $-\text{CH}_3$), 1.45 (d, 3H, $^3J\text{ }6.4\text{ Hz}$, $-\text{CH}_3$), 1.49 (d, 3H, $^3J\text{ }6.6\text{ Hz}$, $-\text{CH}_3$), 1.56 (d, 3H, $^3J\text{ }6.6\text{ Hz}$, $-\text{CH}_3$), 5.05 (septett, 2H, $^3J\text{ }6.6\text{ Hz}$, $-\text{CH}(\text{CH}_3)_2$). $^{13}\text{C NMR}$ (d_6 -acetone, $25\text{ }^{\circ}\text{C}$) δ : 18.6 (CH_3), 21.1 (CH_3), 51.3 (CH), 55.5 (CH), 147.0 (C); (d_6 -acetone, $-65\text{ }^{\circ}\text{C}$) δ : 18.3 (CH_3), 18.3 (CH_3), 21.6 (CH_3), 22.0 (CH_3), 50.8 (CH), 54.9 (CH), 146.9 (C). $^{14}\text{N NMR}$ (d_6 -acetone, $25\text{ }^{\circ}\text{C}$) δ : 13 (N_2 , $\Delta\nu_{1/2} = 666\text{ Hz}$), -11 (N_3 , $\Delta\nu_{1/2} = 571\text{ Hz}$), -36 ($-\text{iPrN-NO}_2$, $\Delta\nu_{1/2} = 24\text{ Hz}$), -56 (N_4 , $\Delta\nu_{1/2} = 435\text{ Hz}$), -130 (N_1 , $\Delta\nu_{1/2} = 201\text{ Hz}$), -200 ($-\text{iPrN-NO}_2$, $\Delta\nu_{1/2} = 989\text{ Hz}$); m/z (CI, *i*-Buten) 215 [(M + H⁺) (18)], 210 (15), 196 (15), 170 (100), 169 (18); m/z (DEI) 169 (37), 154 (12), 127 (24), 126 (10), 110 (9), 111 (36), 99 (10), 86 (39), 85 (11), 14 (84), 80 (29), 69 (14), 64 (15), 58 (22), 57 (16), 48 (19), 43 (100), 42 (21), 41 (30), 39 (9). $\text{C}_7\text{H}_{14}\text{N}_6\text{O}_2$ (214.23): Calcd C, 39.3; H, 6.6; N, 39.2. Found: C, 39.2; H, 6.6; N, 39.4.

7-Nitro-5,6-dihydro-7*H*-imidazo[1,2-*d*]tetrazole (6c). Recrystallization from acetone/water. Mp $150\text{ }^{\circ}\text{C}$ (decomp). $\tilde{\nu}(\text{KBr})$ [cm^{-1}]: 3035 (vw, $-\text{CH}_2$), 3017 (vw, $-\text{CH}_2$), 1592 (vs, $\tilde{\nu}_{\text{asym}} \text{NO}_2$), 1550 (s, $\tilde{\nu} (\text{C}=\text{N})$), 1515 (m), 1472 (m), 1359 (s), 1335 (vs, $\tilde{\nu} \text{-N-N=N}^+$), 1299 (s, $\tilde{\nu}_{\text{sym}} \text{NO}_2$), 1276 (m), 1235 (m), 1204 (m, $\tilde{\nu}$ tetrazole), 1186 (m, $\tilde{\nu}$ tetrazole), 1138 (w, $\tilde{\nu}$ tetrazole), 1108 (vw, $\tilde{\nu}$ tetrazole), 1041 (vw, $\tilde{\nu}$ tetrazole), 956 (w, $\tilde{\nu} \text{-CH}_3\text{N-NO}_2$), 800 (w), 763 (w), 747 (w), 715 (m), 683 (m), 527 (vw). Raman (200 mW) $\tilde{\nu}[\text{cm}^{-1}]$: 3035 (45), 3018 (33), 2995 (52), 2976 (60), 2933 (12), 2902 (14), 1582 (59), 1552 (100, $\tilde{\nu}_{\text{asym}} \text{NO}_2$), 1495 (10), 1471 (37), 1457 (25), 1378 (9), 1363 (18), 1291 (48, $\tilde{\nu} \text{-N-N=N}^+$), 1268 (30), 1235 (60, $\tilde{\nu}_{\text{sym}} \text{NO}_2$), 1207 (26), 1140 (17, $\tilde{\nu}$ tetrazole), 1109 (10, $\tilde{\nu}$ tetrazole), 1042 (60, $\tilde{\nu}$ tetrazole), 957 (12, $\tilde{\nu}$ tetrazole), 935 (21, $\tilde{\nu} \text{-CH}_3\text{N-NO}_2$), 801 (90), 763 (8), 719 (7), 683 (23), 527 (31), 441 (29), 402 (42), 326 (22), 213 (29), 122 (21). $^1\text{H NMR}$ (d_6 -acetone) AA'BB'-spectrum ($\delta_{\text{A}} = 4.85$, $\delta_{\text{B}} = 5.36$, $\text{N} = 29\text{ Hz}$, CH_2). $^{13}\text{C NMR}$ (d_6 -acetone) δ : 42.9 (CH_2), 58.2 (CH_2), 158.6 (C). $^{14}\text{N NMR}$ (d_6 -acetone) δ : 30 (N_3 , $\Delta\nu_{1/2} = 238\text{ Hz}$), -25 (N_2 , $\Delta\nu_{1/2} = 262\text{ Hz}$), -42 ($-\text{RN-NO}_2$, $\Delta\nu_{1/2} = 24\text{ Hz}$), -82 (N_4 , $\Delta\nu_{1/2} = 190\text{ Hz}$), -158 (N_1 , $\Delta\nu_{1/2} = 142\text{ Hz}$), -206 ($-\text{RN-NO}_2$, $\Delta\nu_{1/2} = 476\text{ Hz}$); m/z (DEI) [(M⁺) (34)], 111 (30), 98 (11), 55 (70), 54 (100), 53 (59), 52 (30), 46 (45), 40 (13), 30 (53). $\text{C}_3\text{H}_4\text{N}_6\text{O}_2$ (156.10): Calcd: C, 23.1; H, 2.6; N, 53.8. Found: C, 22.7; H, 2.7; N, 53.6.

X-ray Structure Determinations. X-ray quality single crystals of **3c** (CCDC 269260), **5a** (CCDC 269261), and **6c** (CCDC 269265) were mounted in a Pyrex capillary, and the X-ray crystallographic data were collected on a Nonius Mach3 diffractometer with graphite-monochromated Mo K α radiation ($\lambda = 0.71073\text{ \AA}$). The X-ray crystallographic data for **6a** (CCDC 269263) and **6b** (CCDC 269264) were collected on a STOE IPDS area detector and for **3a** (CCDC 269259) and **5c** (CCDC 269262) data were collected on a Nonius Kappa CCD diffractometer using graphite-monochromated Mo K α radiation ($\lambda = 0.71073\text{ \AA}$). Unit cell parameters for **3c**, **5a**, and **6c** were obtained from setting angles of a minimum of 15 carefully centered reflections having $2\theta > 20^{\circ}$; the choice of the space group was based on systematically absent reflections and confirmed by the successful solution and refinements of the structures. The structures were solved by direct methods (SHELXS-86, SIR97)^{56,57} and refined by means of full-matrix least-squares procedures using SHELXL-97. Empirical absorption correction by Psi-scans was used for **3c**, **5a**, and **6c**. In the case of **3a**, **6a** and **6b** numerical absorption correction by XRed was applied.⁵⁶ Crystal-

(56) (a) Sheldrick, G. M. *SHELXL-86, Program for Solution of Crystal Structures*; University of Göttingen: Göttingen, Germany, 1986. (b) Sheldrick, G. M. *SHELXL-97, Program for Solution of Crystal Structures*; University of Göttingen: Göttingen, Germany, 1997. (c) Gabe, E. J.; Le Page, Y.; Charland, J.-P.; Lee, F. L.; White, P. S. *J. Appl. Crystallogr.* **1989**, *22*, 384. (d) *XRed*, rev. 1.09; Darmstadt, Germany.

(57) Altomare, A.; Burla, M. C. M.; Camalli, M.; Cascarano, G. L.; Giacovazzo, C.; Guagliardi, A.; Moliterni, A. G. G.; Polidori, G.; Spagna, R. *J. Appl. Crystallogr.* **1999**, *32*, 115.

lographic data are summarized in Table S1 (Supporting Information). Selected bond lengths and angles are given in Table S2 (Supporting Information). All non-hydrogen atoms were refined anisotropically. In the case of **3c**, **5a**, and **6c** the hydrogen atoms were included at geometrically idealized positions and refined. They were assigned fixed isotropic temperature factors with the value of $1.2B_{\text{eq}}$ of the atom to which they were bonded. The hydrogen atoms of compound **3a**, **5c**, **6a** and **6b** were located from difference electron-density map and refined isotropically. Further information on the crystal structure determinations (excluding structure factors) has been deposited with the Cambridge Crystallographic Data Centre as supplementary publication nos. 269259, 269260, 269261, 269262, 269263, 269264, and 269265. Copies of the data can be obtained free of charge on application to CCDC, 12 Union Road, Cambridge CB2 1EZ, UK (fax: (+44) 1223-336-033. e-mail: deposit@ccdc.cam.ac.uk).

Acknowledgment. The authors are indebted to and thank Prof. Dr. P. Klüfers for his generous allocation of X-ray diffractometer time. The authors are also indebted to and would like to thank one of the reviewers for his encouraging advice.

Financial support of this work by the University of Munich (LMU) and the Fonds der Chemischen Industrie is gratefully acknowledged. J.J.W. thanks for a FCI Ph.D. fellowship (DO 171/46) and an Alexander von Humboldt postdoctoral scholarship. The authors are also indebted to and like to thank Dr. Claudia Rienäcker for the calorimetric measurements. Financial support by the WIWEB is gratefully acknowledged.

Supporting Information Available: Tables S1–S3 contain structural data and selected geometrical parameter of the investigated species. In Table S4 and S5, WBIs and Mulliken/NBO charges are summarized. The electrostatic potentials (ESP) mapped onto the electronic density surface (single points onto the molecular structure at the B3LYP/6-31G(d,p) level of theory) are shown in Figures S2–S6. Figure S7 show the temperature-dependent ^1H and ^{13}C NMR spectra of **6b**. The total energies and Gibbs free energies of the calculated species are summarized in Tables S6–S8. CIF files. This material is available free of charge via the Internet at <http://pubs.acs.org>.

JO0513820